INORGANIC CHEMISTRY
FRONTIERS

PAPER

Q1

Cite this: DOI: 10.1039/c3qi00083d

Tuning the magnetic behaviors in [$Fe^{III}_{12}Ln^{III}_{4}$] clusters with aromatic carboxylate ligands†

Q2

Sui-Jun Liu, Yong-Fei Zeng, Li Xue, Song-De Han, Ji-Min Jia, Tong-Liang Hu* and Xian-He Bu

Received 9th November 2013,
Accepted 9th January 2014

DOI: 10.1039/c3qi00083d

rsc.li/frontiers-inorganic

A family of $Fe_{12}Ln_4$ clusters based on thiophene-3-carboxylic acid (3-TCA) or 3-methoxybenzoic acid (*m*-MOBA) were synthesized with a *step-by-step* strategy, namely [$Fe_{12}Ln_4(\mu_4\text{-}O)_6(\mu_3\text{-}O)_4(\mu_3\text{-}OH)_4(3\text{-}TCA)_{24}$] (Ln = La (**1**), Gd (**3**) and Dy (**4**)), {[$Fe_{24}Sm_8(\mu_4\text{-}O)_{12}(\mu_3\text{-}O)_8(\mu_3\text{-}OH)_8(3\text{-}TCA)_{46}(NO_3)_2$]·4$CH_3CN$} (**2**), [$Fe_{12}La_4(\mu_4\text{-}O)_6(\mu_3\text{-}O)_4(\mu_3\text{-}OH)_4$(*m*-MOBA)$_{24}$] (**5**) and {[$Fe_{12}Sm_4(\mu_4\text{-}O)_6(\mu_3\text{-}O)_4(\mu_3\text{-}OH)_4$(*m*-MOBA)$_{24}$]·4$CH_3CN$} (**6**). For each of the six complexes, two $Fe_4O_2(OH)_2$ cubane units "sandwich" four Fe^{III} centers to form $Fe_{12}O_{10}(OH)_4$, and it is further connected to four Ln^{III} ions through six μ_4-O^{2-} bridges to obtain a $Fe_{12}Ln_4$ core. Magnetic analyses indicate that **1–6** show different magnetic properties, and **2** and **6** show SMM-like behaviors, due to the differences in lanthanide ions and aromatic monocarboxylate ligands. Note that Sm^{III}-containing 3d–4f clusters exhibiting SMM-like behavior are still rare in the documented cases.

Introduction

In recent years, cluster complexes and coordination polymers based on polynuclear clusters have drawn much attention of researchers, focusing on designing new functional molecular magnetic materials and metal–organic frameworks.[1] Especially, considerable interest has been focused on employing a heterometallic approach to construct clusters and chain based compounds with fascinating magnetic phenomena,[2] such as single-chain magnets (SCMs) behavior[3] and single-molecule magnets (SMMs) behavior,[4] which might be promising candidates for novel functional molecular magnetic materials.[5] The synthesis of SMMs with larger energy barriers and higher blocking temperature has become an area of intensive research activity since the first discovery of SMMs in the 1990s.[6] Usually, SMM behavior results from the favorable arrangement of metal ions with single ion anisotropy in a high-ground-spin state molecule.[7] In the search for enhanced SMMs, the combination of 4f and 3d metal ions has been gradually receiving more and more attention.[8] Additionally, the potential of iron-based systems has long been recognized by chemical researchers for the synthesis of magnetically interesting systems and SMMs.[9] More recently, interesting and unusual magnetic effects have been observed on lanthanide complexes, especially those involving Tb and Dy because of their large anisotropy.[2f,10] Thus, several Fe^{III}–Ln^{III} systems have been documented in order to incorporate favorable properties of both Fe^{III} and Ln^{III} ions (many examples for Ln = Tb/Dy).[11]

Bearing various bridging modes and magnetic exchange pathways between metal centers, carboxylate ligands have been widely used in the construction of 3d complexes with novel structures and interesting magnetic properties.[12] However, pure carboxylate ligands are rarely used for building Fe^{III}–Ln^{III} clusters, due to the great challenge of the synthetic approach.[4a,13] Inspired by a *step-by-step* strategy,[13,14] classic iron-based precursors (Fe_3O clusters) could be firstly synthesized; then Fe_3O precursors as primary reactants react with lanthanide ions to facilitate the cluster formation. By this approach, we have obtained some new bridging networks affording interesting magneto-structural information. The $Fe_{12}Sm_4$ cluster constructed from benzoic acid displaying SMM behavior, which originates from the anisotropy of Sm^{III} ions and is still rare in the documented cases, has been reported by our group.[15] In this work, we chose thiophene-3-carboxylic acid (3-TCA) and 3-methoxybenzoic acid (*m*-MOBA) (Scheme 1) as primary ligands, because not only they are rigid ligands with carboxylate groups to construct high-nuclear clusters but also they are similar to benzoic acid in order to better understand the variations of magnetic behavior of the complexes.

Department of Chemistry, TKL of Metal- and Molecule-Based Material Chemistry and Collaborative Innovation Center of Chemical Science and Engineering (Tianjin), Nankai University, Tianjin 300071, P.R. China. E-mail: tlhu@nankai.edu.cn; Fax: +86-22-23502458

Q3

† Electronic supplementary information (ESI) available. CCDC 894850–894855. For ESI and crystallographic data in CIF or other electronic format see DOI: 10.1039/c3qi00083d

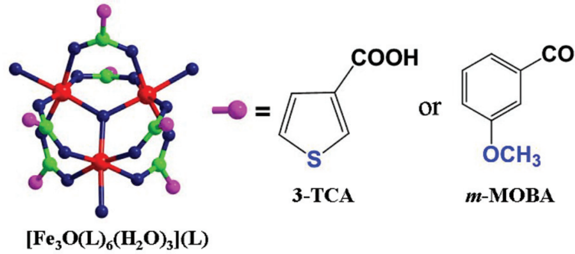

Scheme 1 The structure core of Fe_3O precursor constructed from 3-TCA or *m*-MOBA.

As part of our continuing studies on the synthesis and magnetic properties of Fe–Ln clusters,[15] we report herein a family of $Fe_{12}Ln_4$ clusters from the reaction of 3-TCA/*m*-MOBA and metal ions of iron and lanthanide, namely $[Fe_{12}Ln_4(\mu_4\text{-}O)_6(\mu_3\text{-}O)_4(\mu_3\text{-}OH)_4(3\text{-}TCA)_{24}]$ (Ln = La (**1**), Gd (**3**) and Dy (**4**)), $\{[Fe_{24}Sm_8(\mu_4\text{-}O)_{12}(\mu_3\text{-}O)_8(\mu_3\text{-}OH)_8(3\text{-}TCA)_{46}(NO_3)_2]\cdot 4CH_3CN\}$ (**2**), $[Fe_{12}La_4(\mu_4\text{-}O)_6(\mu_3\text{-}O)_4(\mu_3\text{-}OH)_4(m\text{-}MOBA)_{24}]$ (**5**) and $\{[Fe_{12}Sm_4(\mu_4\text{-}O)_6(\mu_3\text{-}O)_4(\mu_3\text{-}OH)_4(m\text{-}MOBA)_{24}]\cdot 4CH_3CN\}$ (**6**). It is revealed that **2** and **6** show SMM-like behaviors. Interestingly, no SMM-like behaviour for **4** was observed despite the strong anisotropy of Dy^{III} ions. To the best of our knowledge, Sm^{III}-containing 3d–4f clusters exhibiting SMM-like behavior have been reported rarely so far.

Experimental

Materials and measurements

All the starting materials for synthesis were commercially available and used as received. $[Fe_3O(3\text{-}TCA)_6(H_2O)_3](3\text{-}TCA)$ and $[Fe_3O(m\text{-}MOBA)_6(H_2O)_3](m\text{-}MOBA)$ were prepared according to the procedures reported previously with small modifications.[16] Elemental analyses (C, H and N) were performed on a Perkin-Elmer 240C analyzer (Perkin-Elmer, USA). IR spectra were measured on a TENSOR 27 OPUS FT-IR spectrometer using KBr disks dispersed with sample powders in the 4000–400 cm^{-1} range (Bruker, German). Magnetic data were collected using crystals of the samples on a Quantum Design MPMS-XL-7 SQUID magnetometer. The data were corrected using Pascal's constants to calculate the diamagnetic susceptibility, and experimental corrections for the sample holder were applied.

Synthesis of 1–6

$[Fe_{12}La_4(\mu_4\text{-}O)_6(\mu_3\text{-}O)_4(\mu_3\text{-}OH)_4(3\text{-}TCA)_{24}]$ (1). $[Fe_3O(3\text{-}TCA)_6(H_2O)_3](3\text{-}TCA)$ (0.1 mmol) and $La(NO_3)_3\cdot 6H_2O$ (0.1 mmol) were added to 9 mL MeCN solution, stirred for 5 min and transferred to a 23 mL Teflon-lined autoclave and heated to 135 °C for 2 days. After cooling to room temperature, brown crystals were collected. The yield was *ca.* 20% based on La. Anal. calcd for $C_{120}H_{76}Fe_{12}S_{24}O_{62}La_4$ (%): C, 31.99; H, 1.70. Found (%): C, 31.62; H, 2.12. FT-IR (cm^{-1}): 3420w, 3112w, 2170w, 1575m, 1520s, 1438s, 1357s, 878m, 832m, 759s, 694m.

$\{[Fe_{24}Sm_8(\mu_4\text{-}O)_{12}(\mu_3\text{-}O)_8(\mu_3\text{-}OH)_8(3\text{-}TCA)_{46}(NO_3)_2]\cdot 4CH_3CN\}$ (2). A similar procedure as that for **1** was used for this complex except that $La(NO_3)_3\cdot 6H_2O$ was replaced by $Sm(NO_3)_3\cdot 6H_2O$ and the heating temperature was 125 °C. The yield was *ca.* 28% based on Sm. Anal. calcd for $C_{238}H_{158}Fe_{24}S_{46}O_{126}N_6Sm_8$ (%): C, 31.28; H, 1.74; N, 0.92. Found (%): C, 31.79; H, 2.19; N, 1.36. FT-IR (cm^{-1}): 3109w, 2366w, 2330w, 1579s, 1526m, 1438s, 1358s, 873w, 833w, 758s, 697w.

$[Fe_{12}Gd_4(\mu_4\text{-}O)_6(\mu_3\text{-}O)_4(\mu_3\text{-}OH)_4(3\text{-}TCA)_{24}]$ (3). A similar procedure as that for **1** was used for this complex except that $La(NO_3)_3\cdot 6H_2O$ was replaced by $Gd(NO_3)_3\cdot 6H_2O$ and the heating temperature was 140 °C. The yield was *ca.* 25% based on Gd. Anal. calcd for $C_{120}H_{76}Fe_{12}S_{24}O_{62}Gd_4$ (%): C, 31.48; H, 1.67. Found (%): C, 31.03; H, 2.20. FT-IR (cm^{-1}): 3414w, 3118m, 1575s, 1523s, 1442s, 1351s, 1126m, 840m, 758s, 695m, 462m.

$[Fe_{12}Dy_4(\mu_4\text{-}O)_6(\mu_3\text{-}O)_4(\mu_3\text{-}OH)_4(3\text{-}TCA)_{24}]$ (4). A similar procedure as that for **1** was used for this complex except that $La(NO_3)_3\cdot 6H_2O$ was replaced by $Dy(NO_3)_3\cdot 6H_2O$ and the heating temperature was 135 °C. The yield was *ca.* 23% based on Dy. Anal. calcd for $C_{120}H_{76}Fe_{12}S_{24}O_{62}Dy_4$ (%): C, 31.34; H, 1.67. Found (%): C, 31.01; H, 2.09. FT-IR (cm^{-1}): 3364s, 1617s, 1512s, 1462m, 1338s, 842m, 776m, 722m, 648m.

$[Fe_{12}La_4(\mu_4\text{-}O)_6(\mu_3\text{-}O)_4(\mu_3\text{-}OH)_4(m\text{-}MOBA)_{24}]$ (5). $[Fe_3O(m\text{-}MOBA)_6(H_2O)_3](m\text{-}MOBA)$ (0.1 mmol) and $La(NO_3)_3\cdot 6H_2O$ (0.1 mmol) were added to 9 mL MeCN solution, stirred for 5 min and transferred to a 23 mL Teflon-lined autoclave and heated to 130 °C for 2 days. After cooling to room temperature, brown crystals were collected. The yield was *ca.* 23% based on La. Anal. calcd for $C_{192}H_{172}Fe_{12}O_{86}La_4$ (%): C, 45.38; H, 3.41. Found (%): C, 44.97; H, 3.73. FT-IR (cm^{-1}): 3418w, 3132w, 2366w, 1558 s, 1454m, 1406s, 1248m, 1124m, 1037m, 764s, 464m.

$\{[Fe_{12}Sm_4(\mu_4\text{-}O)_6(\mu_3\text{-}O)_4(\mu_3\text{-}OH)_4(m\text{-}MOBA)_{24}]\cdot 4CH_3CN\}$ (6). A similar procedure as that for **5** was used for this complex except that $La(NO_3)_3\cdot 6H_2O$ was replaced by $Sm(NO_3)_3\cdot 6H_2O$ and the heating temperature was 140 °C. The yield was *ca.* ~26% based on Sm. Anal. calcd for $C_{199}H_{181}Fe_{12}N_4O_{86}Sm_4$ (%): C, 45.30; H, 3.45; N, 1.06. Found (%): C, 44.61; H, 3.44; N, 0.59. FT-IR (cm^{-1}): 3358s, 2843w, 2361m, 1567s, 1456s, 1410s, 1284m, 1249m, 1044m, 764s, 465m.

Crystallographic studies

X-ray single-crystal diffraction data for complexes **1–5** and **6** were collected on a SCX-Mini diffractometer at 293(2) K and a Rigaku RAXIS-RAPID diffractometer at 113(2) K with Mo-Kα radiation (λ = 0.71073 Å) by ω scan mode, respectively. The program *CrystalClear*[17] was used for integration of the diffraction profiles. All the structures were solved by direct methods using the SHELXS program of the SHELXTL package and refined by full-matrix least-squares methods with SHELXL (semi-empirical absorption corrections were applied using SADABS program).[18] Metal atoms in complexes **1–6** were located from *E*-maps and other non-hydrogen atoms were located in successive difference Fourier syntheses and refined with anisotropic thermal parameters on F^2. The hydrogen

Table 1 Crystal data and structure refinement parameters for complexes **1–6**

	1	**2**	**3**	**4**	**5**	**6**
Chemical formula	$C_{120}H_{76}Fe_{12}S_{24}O_{62}La_4$	$C_{238}H_{158}Fe_{24}S_{46}N_6O_{126}Sm_8$	$C_{120}H_{76}Fe_{12}S_{24}O_{62}Gd_4$	$C_{120}H_{76}Fe_{12}S_{24}O_{62}Dy_4$	$C_{192}H_{172}Fe_{12}O_{86}La_4$	$C_{199}H_{181}Fe_{12}N_4O_{86}Sm_4$
Formula weight	4505.17	9135.66	4578.55	4599.55	5081.13	5276.08
Crystal system	Monoclinic	Triclinic	Monoclinic	Monoclinic	Triclinic	Triclinic
Space group	$C2/c$	$P\bar{1}$	$C2/c$	$C2/c$	$P\bar{1}$	$P\bar{1}$
a (Å)	29.727(6)	17.441(4)	29.688(6)	29.630(6)	17.982(4)	17.790(3)
b (Å)	27.890(6)	18.664(4)	27.889(6)	27.930(6)	19.269(4)	18.955(3)
c (Å)	20.138(4)	28.858(6)	20.013(4)	19.955(4)	19.494(4)	19.512(4)
$\alpha/°$	90	107.129(3)	90	90	60.62(3)	118.971(11)
$\beta/°$	95.33(3)	91.4500(10)	95.96(3)	96.10(3)	68.77(3)	95.426(17)
$\gamma/°$	90	115.983(4)	90	90	74.31(3)	106.737(13)
$V/Å^3$	16 624(6)	7939(3)	16 480(6)	16 421(6)	5450.5(19)	5293.0(16)
Z	4	1	4	4	1	1
$D_{calcd}/g\ cm^{-3}$	1.798	1.911	1.845	1.860	1.502	1.655
μ/mm^{-1}	2.399	2.903	2.993	3.208	1.622	1.979
T/K	293(2)	293(2)	293(2)	293(2)	293(2)	113(2)
R_{int}	0.1692	0.0339	0.1288	0.1438	0.1365	0.0434
$R^a[I > 2\sigma(I)]$	0.1216	0.0895	0.1023	0.1024	0.1045	0.0533
wR^b[all data]	0.2897	0.2400	0.2437	0.2149	0.2815	0.1623

[a] $R_1 = \sum||F_o| - |F_c||/\sum|F_o|$. [b] $wR_2 = [\sum[w(F_o^2 - F_c^2)^2]/\sum w(F_o^2)^2]^{1/2}$.

atoms of the ligands were generated theoretically onto the specific atoms and refined isotropically with fixed thermal factors. The hydrogen atoms of hydroxyl groups were not assigned. Detailed crystallographic data are summarized in Table 1. CCDC 894850–894855 (complexes **1–6**) contain the supplementary crystallographic data for this paper.

Results and discussion

Synthesis considerations

A *step-by-step* strategy was employed to synthesize six new $Fe_{12}Ln_4$ clusters, which can guide the synthesis of high-nuclear 3d–4f clusters. In the solvothermal reaction, an anhydrous environment is necessary for successfully obtaining target complexes. The starting material is a triangular Fe_3O cluster, but it was transformed into Fe_4O_4 moieties in the final product, which may be facilitated by the addition of $Ln(NO_3)_3$. Besides the method in the Experimental section, we have tried a one-step method to construct target clusters. Unfortunately, no single crystals were afforded for structural analysis in our efforts to prepare the clusters. Notably, the synthetic temperatures and yields of **1–6** have some small differences and their stabilities are not very good.

Structural characterization

Complexes **1–4** and **5–6** are isostructural, respectively, with a similar structure as in the reported study[15] by our group, although complex **2** consists of two different $[Fe_{12}Sm_4]$ clusters, one containing 24 3-TCA ligands and another including 22 3-TCA ligands and 2 NO_3^- anions. Therefore, herein only the structure of **3** is described briefly. Single-crystal X-ray diffraction analysis reveals that complex **3** crystallizes in the $C2/c$ space group. The asymmetric unit of **3** consists of six Fe^{III} ions, two Gd^{III} ions, three μ_4-O^{2-} anions, two μ_3-O^{2-} anions, two μ_3-OH groups and twelve 3-TCA ligands. The ranges of Gd–O and Fe–O bond lengths are 2.323(10)–2.551(9) Å and 1.816(9)–2.111(10) Å, respectively, and O–Gd–O and O–Fe–O angles fall in the ranges of 67.5(3)–146.0(4)° and 80.9(4)–168.2(5)°. Each of the Fe^{III} ions has a distorted octahedral coordination geometry and all of the Gd^{III} ions are in a distorted square-antiprism fashion. As shown in Fig. 1a and 1c, two μ_3-OH^- and two O^{2-} anions bridge four Fe^{III} ions to form $Fe_4O_2(OH)_2$ cubane units, and two of these cubane units "sandwich" four central Fe^{III} ions *via* four μ_3-O^{2-} bridges. The connection of two cubane units and one central Fe_4 unit forms a $Fe_{12}O_{10}(OH)_4$ core along with the two $Fe_4O_2(OH)_2$ cubane units. Further, four Gd^{III} ions are linked to $Fe_{12}O_{10}(OH)_4$ through six μ_4-O^{2-} anions, forming the $Fe_{12}Gd_4$ core of **3**. In other words, the four Gd^{III} ions are linked between the cubanes and the central Fe_4 group. In addition, twenty η^1:η^1-μ_2-3-TCA ligands and four η^1:η^2-μ_3-3-TCA ligands occupy the periphery of the $Fe_{12}Gd_4$ core and complete the coordination spheres of the Fe^{III} and Gd^{III} centers by the O atoms of the carboxylate group. The molecular structure of **6** based on *m*-MOBA is shown in Fig. 1b.

Magnetic properties

Magnetic measurements were carried out on crystalline samples of **1–6** and their magnetic properties were investigated by solid state magnetic susceptibility measurements in the 2–300 K range at 1 kOe field and the isothermal field-dependent magnetizations $M(H)$ at fields up to 50/70 kOe. The alternating current (ac) susceptibility measurements for **2**, **4** and **6** were performed at low temperatures under H_{dc} = 0 Oe and H_{ac} = 3.5 Oe for variable frequencies (from 1488 Hz to 3 Hz). Despite the fact that they contain a similar structure, they show varying magnetic behaviors as discussed below.

The magnetic properties in the form of $\chi_M T$ *vs.* T plots of **1–6** are shown in Fig. 2. Because **1** and **5** contain diamagnetic

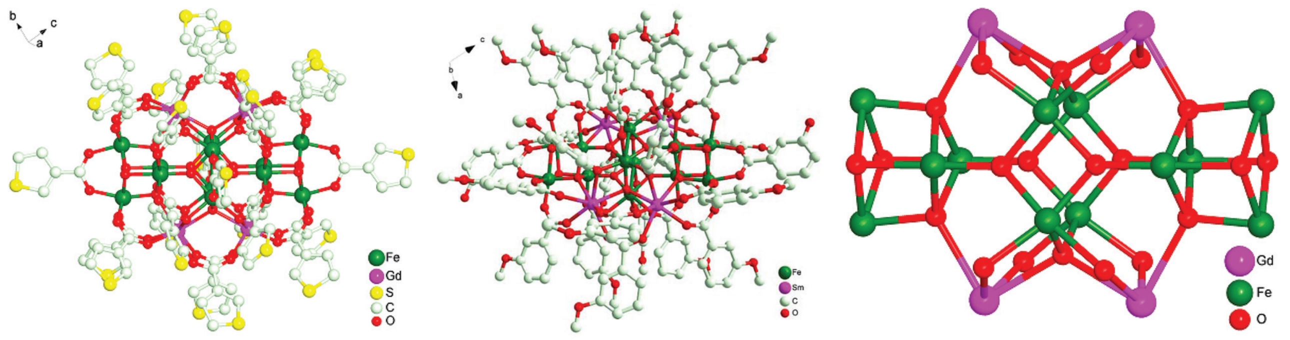

(a) (b) (c)

Fig. 1 (a) The molecular structure of **3**; (b) the molecular structure of **6**; (c) the $Fe_{12}Gd_4$ core of **3**.

La^{III} ions, they can be simplified as a Fe_{12} core from the magnetic point of view. For **1** and **5**, the $\chi_M T$ values are 22.49 and 20.90 emu mol^{-1} K at 300 K, respectively, which are much lower than the expected value of 52.5 emu mol^{-1} K for twelve Fe^{III} ions (S = 5/2, g = 2) suggesting dominant antiferromagnetic (AF) interactions between Fe^{III} ions in **1** and **5**.[2f] As the temperature decreases, the value of $\chi_M T$ slowly decreases down to a minimum value of 19.31 emu mol^{-1} K at 120 K for **1** and 19.11 emu mol^{-1} K at 140 K for **5**, further indicating AF coupling between metal centres. Upon lowering the temperature to 3.5 K and 7 K, $\chi_M T$ abruptly increases to the maximum values (39.91 and 36.82 emu mol^{-1} K, respectively), showing ferromagnetic (F) interactions between Fe^{III} ions in **1** and **5**. Further cooling the temperature, $\chi_M T$ decreases down to the minimum values of 39.31 and 34.47 emu mol^{-1} K at 2 K. It is noteworthy that in the temperature range 2–300 K both F and AF interactions exist in the Fe_{12} core of **1** and **5** but at a specific temperature only one is dominant given that the Fe–O–Fe angles are about 95° and 130°.

For **2** and **6**, the values for $\chi_M T$ at 300 K are 21.12 and 20.99 emu mol^{-1} K, much lower than the theoretical value of 52.86 emu mol^{-1} K for four Sm^{III} ($^6H_{5/2}$, L = 5, g = 2/7) and twelve Fe^{III} ions,[15,19] which indicates strong AF coupling between metal centers. The $\chi_M T$ values decrease gradually until 95 and 140 K, reaching 19.55 and 19.51 emu mol^{-1} K, respectively. When the temperature decreases, the $\chi_M T$ values increase, reaching maximum values of 41.32 and 38.40 emu mol^{-1} K at 5 and 6 K, respectively. The $\chi_M T$ products then decrease with a further lowering of the temperature and attain values of 38.59 and 36.68 emu mol^{-1} K at 2 K because of zero-field splitting and/or AF interaction among $Fe_{12}Sm_4$ clusters. As a result, both F and AF interactions exist between metal ions.

For **3**, the value for $\chi_M T$ at room temperature is 50.32 emu mol^{-1} K, much lower than the theoretical value of 84.02 emu mol^{-1} K for four Gd^{III} ($^8H_{7/2}$, L = 0, g = 2) and twelve Fe^{III} ions, which indicates strong AF coupling between metal centers. Upon cooling, the $\chi_M T$ value remains nearly constant, reaching 49.89 emu mol^{-1} K at 18 K, and then decreases rapidly to a value of 20.35 emu mol^{-1} K at 2 K. This is because dominant AF interaction among $Fe_{12}Gd_4$ clusters exists in **3**. For **4**, the value for $\chi_M T$ at room temperature is 82.45 emu mol^{-1} K, lower than the theoretical value of 109.18 emu mol^{-1} K for four Dy^{III} ($^6H_{15/2}$, L = 5, g = 3/4) and twelve Fe^{III} ions, which indicates strong AF coupling between metal ions. Upon cooling, the $\chi_M T$ value linearly decreases, reaching 75.84 emu mol^{-1} K at 22 K, and then decreases rapidly to a value of 45.07 emu mol^{-1} K at 2 K. This is attributed to dominant AF interaction among $Fe_{12}Dy_4$ clusters.

The *M vs. H* curves (at 2 K) for **1–6** are shown in Fig. 3. For **1**, the magnetization at 2 K tends to saturation values of $17.37N\beta$ at 50 kOe and the experimental magnetization curve is below the red line that presents the Brillouin function for S = 8 ground state with g = 2.1, confirming again the existence of AF coupling between the Fe^{III} ions (Fig. S1, ESI†). The magnetization for **5** is familiar to that for **1**. For **2** and **6**, M increases quickly at very low field. In the high field region the increase of magnetization is slow, reaching 19.03 and $19.09N\beta$ at 50 kOe, which are consistent with the theoretical saturated value of $18.89N\beta$. For **3**, M increases linearly at low field and reaches $46.19N\beta$ at 50 kOe, which is a little higher than the theoretical value of $44.04N\beta$. The *M vs. H* curve of **4** is similar to that of **3**. The magnetizations for **2**, **3**, **4** and **6** at 2 K tend to saturation values that may be ascribed to weak AF interactions between Fe^{III} ions and Ln^{III} ions.

Table 2 shows susceptibility data at 300 K for the $Fe_{12}Ln_4$ series of **1–6**. $\Delta\chi_M T$, the contribution to the $\chi_M T$ value of the Ln_4 part in $Fe_{12}Ln_4$, is calculated as $\chi_M T$ ($Fe_{12}Ln_4$) − $\chi_M T$ (**1** or **5**). For **2**, the $\Delta\chi_M T$ value is −1.37 emu mol^{-1} K, which indicates AF coupling between Sm^{III} ions and Fe^{III} ions at 300 K. For **3** and **4**, the $\Delta\chi_M T$ values at 300 K are far below than that expected for a Fe_{12} unit and four Gd^{III}/Dy^{III} ions, indicating that the magnetic exchange interactions between the Gd^{III}/Dy^{III} and Fe^{III} ions are very weak. For **6**, the $\Delta\chi_M T$ value is almost zero, which suggests that the magnetic interactions between Gd^{III} and Gd^{III}/Fe^{III} ions at room temperature are negligible.

In order to elucidate possible SMM behavior, ac measurements for **2**, **4** and **6** were performed. Ac susceptibility measurements for **2** and **6** indicate that whereas the in-phase curves (χ') at high temperature are almost consistent above

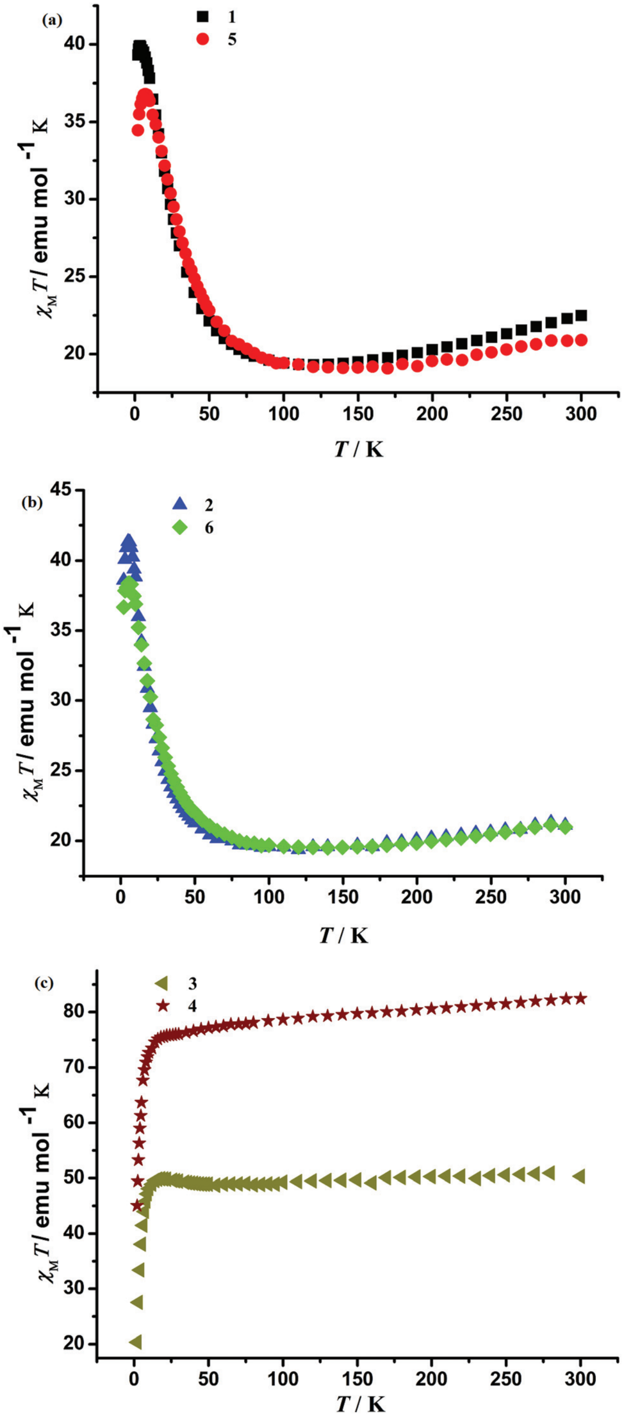

Fig. 2 Temperature dependence of magnetic susceptibilities in the forms of $\chi_M T$ at an applied field of 1 kOe for **1–6**.

3 K, peaks arise below 3 K, and a frequency dependent out-of-phase signal appears, indicating a slow relaxation behavior of the magnetization (Fig. 4). However, the maximum value of χ'' was not observed even at the low temperature (2 K) and high frequency (1488 Hz) due to the limit of the magnetometer. The pre-exponential factor (τ_0) and energy barrier (U) to reverse the magnetization can be roughly estimated from the $\ln(\chi''_M/\chi'_M)$ *vs.* $1/T$ plot at 997 Hz for **2** and 1488 Hz for **6** by considering a single relaxation time (Fig. S2, ESI†). The least-squares fitting of the experimental data through the expression $\chi''_M/\chi'_M = 2\pi\upsilon\tau_0 \exp(U/k_BT)$ gave $\tau_0 \approx 5.9 \times 10^{-8}$ s and $U \approx 9.8$ K for **2**, and $\tau_0 \approx 1.0 \times 10^{-7}$ s and $U \approx 8.7$ K for **6**, respectively. The ac signals suggest the prevalence of quantum tunnelling effect at low temperature. Due to the absence of out-of-phase ac signals in **1** and **5** (Fig. S3, ESI†), the slow magnetic relaxation in **2** and **6** can be attributed to magnetic anisotropy induced by the introduction of Sm^{III} ions with unquenched spin–orbit coupling.

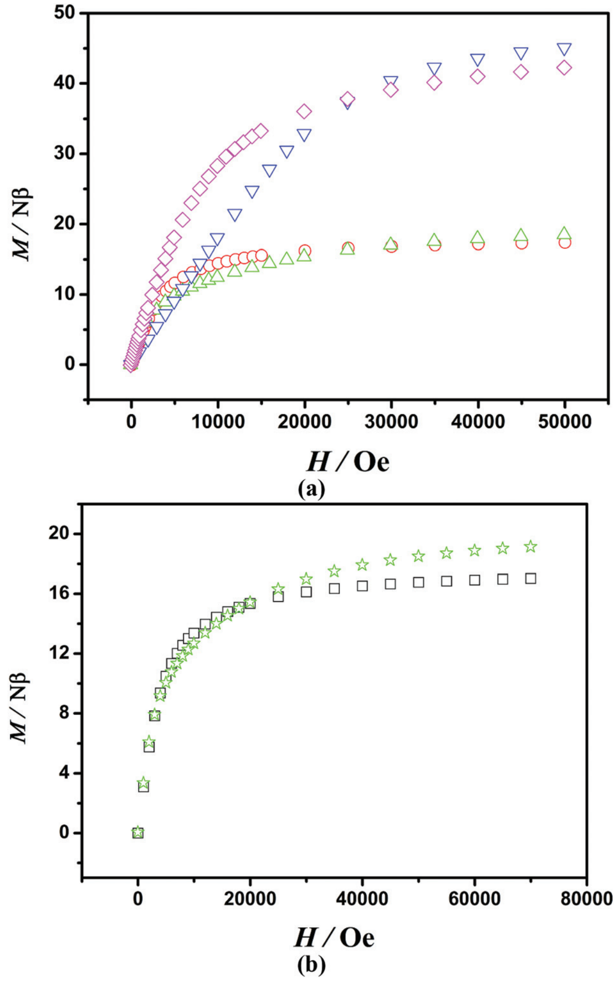

Fig. 3 The *M vs. H* plots at 2 K for **1** (○), **2** (△), **3** (▽), **4** (◇), **5** (□) and **6** (☆).

Because slow relaxation of magnetization is experimentally observed only over a short range of temperatures and no maximum of χ'' is found at the low temperatures technically available, the estimation of these characteristic parameters might not be very accurate, but τ_0 values are consistent with the expected values ($\tau_0 = 10^{-6}$–10^{-11} s) for SMMs.[20] Ac susceptibility measurement for **4** indicates that whereas all the in-phase curves (χ') are almost consistent without peaks, a weak frequency dependent out-of-phase signal appears, indicating a slow relaxation behavior of the magnetization (Fig. S4, ESI†). The energy barrier and characteristic relaxation time could not

Table 2 Susceptibility data for the $Fe_{12}Ln_4$ series of **1–6**. Units: emu mol^{-1} K

	$Fe_{12}La_4$ (**1**)	$Fe_{12}Sm_4$ (**2**)	$Fe_{12}Gd_4$ (**3**)	$Fe_{12}Dy_4$ (**4**)	$Fe_{12}La_4$ (**5**)	$Fe_{12}Sm_4$ (**6**)
4 × (Ln) contribution	—	1.44	31.5	56.68	—	1.44
Theoretical $\chi_M T$ (300 K)	52.5	53.9	84.0	109.18	52.5	53.9
Experimental $\chi_M T$ (300 K)	22.49	21.12	50.32	82.45	20.90	20.99
$\Delta\chi_M T^a$	—	−1.37	+27.83	+59.96	—	+0.09

[a] $\Delta\chi_M T$ (**2**/**3**/**4**) = $\chi_M T$ ($Fe_{12}Ln_4$) − $\chi_M T$ ($Fe_{12}La_4$, **1**) of experimental values. $\Delta\chi_M T$ (**6**) = $\chi_M T$ ($Fe_{12}Sm_4$, **6**) − $\chi_M T$ ($Fe_{12}La_4$, **5**).

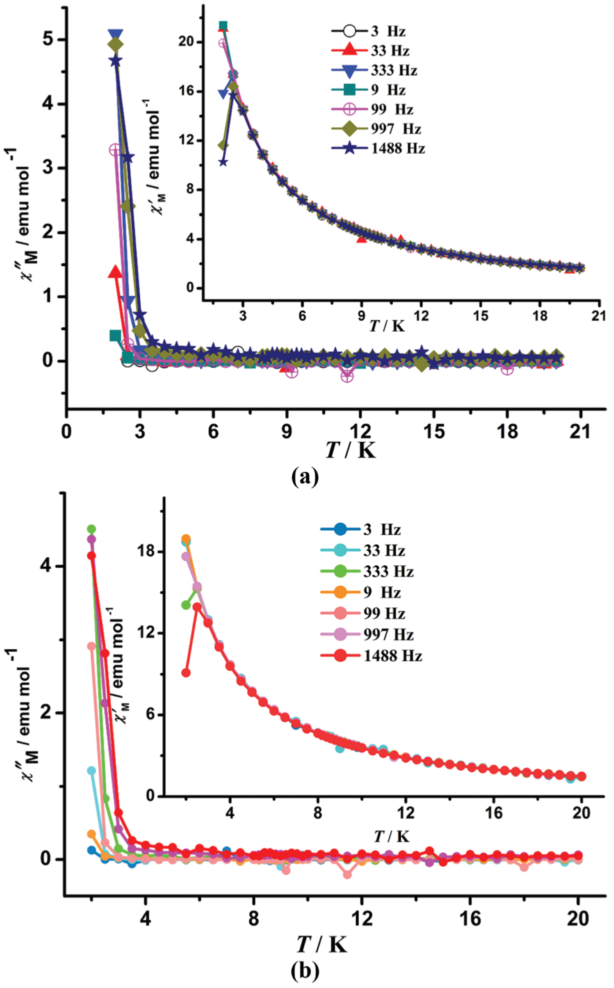

Fig. 4 Temperature dependence of the ac χ_M at different frequencies with H_{dc} = 0 Oe for **2** (a) and **6** (b).

be obtained because the maximum value of χ'' was not found due to the 2 K temperature limit of the instrument. Therefore, slow magnetic relaxation behaviors for **2**, **4** and **6** were observed, and **2** and **6** exhibit SMM-like properties. Notably, Sm^{III}-containing complexes displaying SMM-like behaviors are rare because the anisotropy of Sm^{III} ions is weaker than that of other anisotropic lanthanide ions such as Tb^{III} and Dy^{III} ions. Additionally, compared with the first Sm^{III} SMM $Fe_{12}Sm_4$ cluster derived from benzoic acid,[15] complexes **2** and **6** exhibit SMM-like behaviors because of the relatively high measurement temperatures (above 2 K).

Conclusions

In summary, we present here six new $Fe_{12}Ln_4$ clusters synthesized with a *step-by-step* strategy. Varying magnetic properties of the six complexes may result from distinct monocarboxylate ligands and 4f metal ions. Ac magnetic measurements show frequency dependence of the out-of-phase magnetic susceptibility (χ'') suggesting slow relaxation of the magnetization for **2**, **4** and **6**. No obvious χ'' peak but strong field-dependent χ' and χ'' signals can be found, suggesting SMM-like properties for **2** and **6**, and the existence of zero-field quantum tunnelling at low temperature. Therefore, the series study of $Fe_{12}Ln_4$ clusters provides a good example for the construction of high-nuclear Fe–Ln clusters with different magnetic behaviors.

Acknowledgements

This work was financially supported by NSFC (21371102 and 21003078), the NSF of Tianjin, China (11JCYBJC04100) and the Foundation of State Key Laboratory of Coordination Chemistry.

Notes and references

1 (*a*) S. Xiang, Y. He, Z. Zhang, H. Wu, W. Zhou, R. Krishna and B. Chen, *Nat. Commun.*, 2012, **3**, 954; (*b*) Q. Chen, Z. Chang, W. C. Song, H. Song, H. B. Song, T. L. Hu and X. H. Bu, *Angew. Chem., Int. Ed.*, 2013, **52**, 11550–11553; (*c*) S. D. Han, W. C. Song, J. P. Zhao, Q. Yang, S. J. Liu, Y. Li and X. H. Bu, *Chem. Commun.*, 2013, **49**, 871–873; (*d*) Z. B. Han, R. Y. Lu, Y. F. Liang, Y. L. Zhou, Q. Chen and M. H. Zeng, *Inorg. Chem.*, 2012, **51**, 674–679; (*e*) R. J. Wei, Q. Huo, J. Tao, R. B. Huang and L. S. Zheng, *Angew. Chem., Int. Ed.*, 2011, **50**, 8940–8943; (*f*) J. P. Tong, F. Shao, J. Tao, R. B. Huang and L. S. Zheng, *Inorg. Chem.*, 2011, **50**, 2067–2069.

2 (*a*) R. Sessoli and A. K. Powell, *Coord. Chem. Rev.*, 2009, **253**, 2328–2341; (*b*) M. Mannini, F. Pineider, P. Sainctavit, C. Danieli, E. Otero, C. Sciancalepore, A. M. Talarico, M. A. Arrio, A. Cornia, D. Gatteschi and R. Sessoli, *Nat. Mater.*, 2009, **8**, 194–197; (*c*) F. Pointillart, K. Bernot, R. Sessoli and D. Gatteschi, *Chem.–Eur. J.*, 2007, **13**, 1602–1609; (*d*) W. G. Wang, A. J. Zhou, W. X. Zhang, M. L. Tong, X. M. Chen, M. Nakano, C. C. Beedle and D. N. Hendrickson, *J. Am. Chem. Soc.*, 2007, **129**, 1014–

1015; (*e*) P. L. Feng, C. C. Beedle, C. Koo, W. Wernsdorfer, M. Nakano, S. Hill and D. N. Hendrickson, *Inorg. Chem.*, 2008, **47**, 3188–3204; (*f*) A. Baniodeh, I. J. Hewitt, V. Mereacre, Y. H. Lan, G. Novitchi, C. E. Anson and A. K. Powell, *Dalton Trans.*, 2011, **40**, 4080–4086; (*g*) S. J. Liu, W. C. Song, L. Xue, S. D. Han, Y. F. Zeng, L. F. Wang and X. H. Bu, *Sci. China, Ser. B: Chem.*, 2012, **55**, 1064–1072; (*h*) S. D. Jiang, B. W. Wang, H. L. Sun, Z. M. Wang and S. Gao, *J. Am. Chem. Soc.*, 2011, **133**, 4730–4733; (*i*) L. Q. Wei, K. Zhang, Y. C. Feng, Y. H. Wang, M. H. Zeng and M. Kurmoo, *Inorg. Chem.*, 2011, **50**, 7274–7283.

3 (*a*) T. S. Venkatakrishnan, S. Sahoo, N. Bréfuel, C. Duhayon, C. Paulsen, A. L. Barra, S. Ramasesha and J. P. Sutter, *J. Am. Chem. Soc.*, 2010, **132**, 6047–6056; (*b*) I. Bhowmick, E. A. Hillard, P. Dechambenoit, C. Coulon, T. D. Harris and R. Clérac, *Chem. Commun.*, 2012, **48**, 9717–9719; (*c*) J. Ferrando-Soria, D. Cangussu, M. Eslava, Y. Journaux, R. Lescouëzec, M. Julve, F. Lloret, J. Pasán, C. Ruiz-Pérez, E. Lhotel, C. Paulsen and E. Pardo, *Chem.–Eur. J.*, 2011, **17**, 12482–12494.

4 (*a*) V. M. Mereacre, A. M. Ako, R. Clérac, W. Wernsdorfer, G. Filoti, J. Bartolomé, C. E. Anson and A. K. Powell, *J. Am. Chem. Soc.*, 2007, **129**, 9248–9249; (*b*) G. Novitchi, W. Wernsdorfer, L. F. Chibotaru, J. P. Costes, C. E. Anson and A. K. Powell, *Angew. Chem., Int. Ed.*, 2009, **48**, 1614–1619; (*c*) A. Okazawa, T. Nogami, H. Nojiri and T. Ishida, *Inorg. Chem.*, 2008, **47**, 9763–9765; (*d*) Y. Y. Zhu, C. Cui, Y. Q. Zhang, J. H. Jia, X. Guo, C. Gao, K. Qian, S. D. Jiang, B. W. Wang, Z. M. Wang and S. Gao, *Chem. Sci.*, 2013, **4**, 1802–1806.

5 (*a*) S. Nayak, O. Roubeau, S. J. Teat, C. M. Beavers, P. Gamez and J. Reedijk, *Inorg. Chem.*, 2010, **49**, 216–221; (*b*) X. J. Kong, Y. P. Ren, W. X. Chen, L. S. Long, Z. P. Zheng, R. B. Huang and L. S. Zheng, *Angew. Chem., Int. Ed.*, 2008, **47**, 2398–2401; (*c*) X. J. Kong, Y. P. Ren, L. S. Long, Z. P. Zheng, R. B. Huang and L. S. Zheng, *J. Am. Chem. Soc.*, 2007, **129**, 7016–7017; (*d*) C. Benelli and D. Gatteschi, *Chem. Rev.*, 2002, **102**, 2369–2388.

6 (*a*) T. C. Stamatatos, S. J. Teat, W. Wernsdorfer and G. Christou, *Angew. Chem., Int. Ed.*, 2009, **48**, 521; (*b*) I. R. Jeon and R. Clérac, *Dalton Trans.*, 2012, **41**, 9569–9586; (*c*) J. W. Sharples, Y. Z. Zheng, F. Tuna, E. J. L. McInnes and D. Collison, *Chem. Commun.*, 2011, **47**, 7650–7652; (*d*) Y. L. Miao, J. L. Liu, J. Y. Li, J. D. Leng, Y. C. Ou and M. L. Tong, *Dalton Trans.*, 2011, **40**, 10229–10236; (*e*) Y. N. Guo, G. F. Xu, W. Wernsdorfer, L. Ungur, Y. Guo, J. K. Tang, H. J. Zhang, L. F. Chibotaru and A. K. Powell, *J. Am. Chem. Soc.*, 2011, **133**, 11948–11951.

7 (*a*) H. L. C. Feltham, R. Clérac, A. K. Powell and S. Brooker, *Inorg. Chem.*, 2011, **50**, 4232–4234; (*b*) A. Mishra, A. J. Tasiopoulos, W. Wernsdorfer, K. A. Abboud and G. Christou, *Inorg. Chem.*, 2007, **46**, 3105–3115; (*c*) S. K. Langley, L. Ungur, N. F. Chilton, B. Moubaraki, L. F. Chibotaru and K. S. Murray, *Chem.–Eur. J.*, 2011, **17**, 9209–9218; (*d*) T. Kajiwara, M. Nakano, K. Takahashi, S. Takaishi and M. Yamashita, *Chem.–Eur. J.*, 2011, **17**, 196–205.

8 (*a*) V. Mereacre, A. Baniodeh, C. E. Anson and A. K. Powell, *J. Am. Chem. Soc.*, 2011, **133**, 15335–15337; (*b*) V. Mereacre, Y. H. Lan, R. Clérac, A. M. Ako, W. Wernsdorfer, G. Buth, C. E. Anson and A. K. Powell, *Inorg. Chem.*, 2011, **50**, 12001–12009; (*c*) C. Aronica, G. Pilet, G. Chastanet, W. Wernsdorfer, J. F. Jacquot and D. Luneau, *Angew. Chem., Int. Ed.*, 2006, **45**, 4659–4662.

9 (*a*) D. Gatteschi, R. Sessoli and A. Cornia, *Chem. Commun.*, 2000, 725–732; (*b*) R. Bagai, M. R. Daniels, K. A. Aboud and G. Christou, *Inorg. Chem.*, 2008, **47**, 3318–3327; (*c*) L. F. Jones, A. Batsanov, E. K. Brechin, D. Collison, M. Helliwell, T. Mallah, E. J. L. McInnes and S. Piligkos, *Angew. Chem., Int. Ed.*, 2002, **41**, 4318–4321; (*d*) L. F. Jones, P. Jensen, B. Moubaraki, K. J. Berry, J. F. Boas, J. R. Pibrow and K. S. Murray, *J. Mater. Chem.*, 2006, **16**, 2690–2697; (*e*) D. M. Low, L. F. Jones, A. Bell, E. K. Brechin, T. Mallah, E. Riviére, S. J. Teat and E. J. L. McInnes, *Angew. Chem., Int. Ed.*, 2003, **42**, 3781–3784; (*f*) H. Oshio, N. Hoshino and T. Ito, *J. Am. Chem. Soc.*, 2000, **122**, 12602–12603.

10 (*a*) Y. Z. Zheng, Y. H. Lan, C. E. Anson and A. K. Powell, *Inorg. Chem.*, 2008, **47**, 10813–10815; (*b*) P. H. Lin, T. J. Burchell, L. Ungur, L. F. Chibotaru, W. Wernsdorfer and M. Murugesu, *Angew. Chem., Int. Ed.*, 2009, **48**, 9489–9492; (*c*) S. J. Liu, J. P. Zhao, W. C. Song, S. D. Han, Z. Y. Liu and X. H. Bu, *Inorg. Chem.*, 2013, **52**, 2103–2109.

11 (*a*) V. Mereacre, D. Prodius, Y. H. Lan, C. Turta, C. E. Anson and A. K. Powell, *Chem.–Eur. J.*, 2011, **17**, 123–128; (*b*) S. Mukherjee, M. R. Daniels, R. Bagai, K. A. Abboud, G. Christou and C. Lampropoulos, *Polyhedron*, 2010, **29**, 54–65.

12 (*a*) Y. Q. Wang, X. M. Zhang, X. B. Li, B. W. Wang and E. Q. Gao, *Inorg. Chem.*, 2011, **50**, 6314–6322; (*b*) Y. W. Li, J. P. Zhao, L. F. Wang and X. H. Bu, *CrystEngComm*, 2011, **13**, 6002–6006; (*c*) Y. W. Li, J. R. Li, L. F. Wang, B. Y. Zhou, Q. Chen and X. H. Bu, *J. Mater. Chem. A*, 2013, **1**, 495–499.

13 A. M. Ako, V. Mereacre, R. Clérac, I. J. Hewitt, Y. H. Lan, C. E. Anson and A. K. Powell, *Dalton Trans.*, 2007, 5245–5247.

14 D. Schray, G. Abbas, Y. H. Lan, V. Mereacre, A. Sundt, J. Dreiser, O. Waldmann, G. E. Kostakis, C. E. Anson and A. K. Powell, *Angew. Chem., Int. Ed.*, 2010, **49**, 5185–5188.

15 Y. F. Zeng, G. C. Xu, X. Hu, Z. Chen, X. H. Bu, S. Gao and E. C. Sañudo, *Inorg. Chem.*, 2010, **49**, 9734–9736.

16 R. F. Weinland and A. Herz, *Ber. Dtsch. Chem. Ges.*, 1912, **45**, 2662.

17 Rigaku, *Process-Auto*, Rigaku Americas Corporation, The Woodlands, Texas, 1998. Q6

18 G. M. Sheldrick, *SHELXTL NT Version 5.1. Program for Solution and Refinement of Crystal Structures*, University of Göttingen, Germany, 1997.

19 S. Sanz, K. Ferreira, R. D. McIntosh, S. J. Dalgarno and E. K. Brechin, *Chem. Commun.*, 2011, **47**, 9042–9044.

20 (*a*) B. Joarder, A. K. Chaudhari, G. Rogez and S. K. Ghosh, *Dalton Trans.*, 2012, **41**, 7695–7699; (*b*) Y. D. Luo, G. M. Sun, D. M. Li and F. Luo, *Inorg. Chem. Commun.*, 2011, **14**, 778–785; (*c*) Z. H. Zhang, Y. Song, T. A. Okamura, Y. Hasegawa, W. Y. Sun and N. Ueyama, *Inorg. Chem.*, 2006, **45**, 2896–2902.